Journal of Ethnopharmacology 257 (2020) 112796

Contents lists available at ScienceDirect

Journal of Ethnopharmacology

journal homepage: www.elsevier.com/locate/jethpharm

Effective-component compatibility of Bufei Yishen formula II inhibits mucus hypersecretion of chronic obstructive pulmonary disease rats by regulating EGFR/PI3K/mTOR signaling

Jiansheng Li[a,b,*,1], Jindi Ma[a,b,1], Yange Tian[a,b], Peng Zhao[a,b], Xuefang Liu[a,b], Haoran Dong[a,b], Wanchun Zheng[a,b], Suxiang Feng[a,b], Lanxi Zhang[a,b], Mingming Wu[a,b], Lihua Zhu[a,b], Shuai Liu[a,b], Di Zhao[a,b]

[a] Co-construction Collaborative Innovation Center for Chinese Medicine and Respiratory Diseases by Henan & Education Ministry of P.R., 450046, China
[b] Henan Key Laboratory of Chinese Medicine for Respiratory Disease, Henan University of Chinese Medicine, Zhengzhou, Henan, 450046, China

ARTICLE INFO

Keywords:
Bufei yishen formula
Chronic obstructive pulmonary disease
Mucus hypersecretion
Effective-component compatibility

Chemical compounds studied in this article:
Paeonol (PubChem CID: 11092)
Icariin (PubChem CID: 5318997)
Nobiletin (PubChem CID: 72344)
Astragaloside IV (PubChem CID: 13943297)
Peiminine (PubChem CID: 167691)
Schisandrin B (PubChem CID: 158103)
Hesperidin (PubChem CID: 10621)
Paeoniflorin (PubChem CID: 442534)
Formalin (PubChem CID: 712)
Ethanol (PubChem CID: 702)
Xylene (PubChem CID: 7237)
Phosphate-buffered saline (PubChem CID: 24978514)
Formaldehyde (PubChem CID: 712)

ABSTRACT

Ethnopharmacological relevance: The effective-component compatibility of Bufei Yishen formula I (ECC-BYF I), a combination of 10 compounds, including total ginsenosides, astragaloside IV, icariin, and paeonol, etc., is derived from Bufei Yishen formula (BYF). The efficacy and safety of ECC-BYF I is equal to BYF. However, the composition of ECC-BYF I needs to be further optimized. Based on the beneficial effects of BYF and ECC-BYF I on chronic obstructive pulmonary disease (COPD), this study aimed to optimize the composition of ECC-BYF I and to explore the effects and mechanisms of optimized ECC-BYF I (ECC-BYF II) on mucus hypersecretion in COPD rats.

Materials and methods: ECC-BYF I was initially optimized to six groups: optimized ECC-BYF I (OECC-BYF I)-A∼F. Based on a COPD rat model, the effects of OECC-BYF I-A∼F on COPD rats were evaluated. R-value comprehensive evaluation was used to evaluate the optimal formula, which was named ECC-BYF II. The changes in goblet cells and expression of mucins and the mRNA and proteins involved in the epidermal growth factor receptor/phosphoinositide-3-kinase/mammalian target of rapamycin (EGFR/PI3K/mTOR) pathway were evaluated to explore the effects and mechanisms of ECC-BYF II on mucus hypersecretion.

Results: ECC-BYF I and its six optimized groups, OECC-BYF I-A∼F, had beneficial effects on COPD rats in improving pulmonary function and lung tissue pathology, reducing inflammation and oxidative stress, and improving the protease/anti-protease imbalance and collagen deposition. R-value comprehensive evaluation found that OECC-BYF I-E (paeonol, icariin, nobiletin, total ginsenoside, astragaloside IV) was the optimal formula for improving the comprehensive effects (lung function: V_T, MV, PEF, EF50, FVC, FEV 0.1, FEV 0.1/FVC; histological changes: MLI, MAN; IL-1β, IL-6, TNF-α, MMP-9, TIMP-1, T-AOC, LPO, MUC5AC, Collagen I and Collagen III). OECC-BYF I-E was named ECC-BYF II. Importantly, the effect of ECC-BYF II showed no significant difference from BYF and ECC-BYF I. ECC-BYF II inhibited mucus hypersecretion in COPD rats, which manifested as reducing the expression of MUC5AC and MUC5B and the hyperplasia rate of goblet cells. The mRNA and protein expression levels of EGFR, PI3K, Akt, and mTOR were increased in COPD rats and were obviously downregulated after ECC-BYF II administration.

Conclusion: ECC-BYF II, which consists of paeonol, icariin, nobiletin, total ginsenoside and astragaloside IV, has beneficial effects equivalent to BYF and ECC-BYF I on COPD rats. ECC-BYF II significantly inhibited mucus hypersecretion, which may be related to the regulation of the EGFR/PI3K/mTOR pathway.

* Corresponding author. Longzihu University Town, Zhengdong New District, Zhengzhou, 450046, Henan, China.
E-mail addresses: li_js8@163.com (J. Li), 15937143260@163.com (J. Ma), yange0910@126.com (Y. Tian), zhaopeng871@126.com (P. Zhao), liuxf0213@163.com (X. Liu), haoranxc@163.com (H. Dong), wanchunzheng@126.com (W. Zheng), fengsx221@163.com (S. Feng), 13140101013@163.com (L. Zhang), hnwumingming@163.com (M. Wu), 15225146823@163.com (L. Zhu), 1012317229@qq.com (S. Liu), zhaodiabcd@sina.com (D. Zhao).
[1] These authors contributed equally to this work and should be considered co-first authors.

https://doi.org/10.1016/j.jep.2020.112796
Received 31 October 2019; Received in revised form 7 March 2020; Accepted 23 March 2020
Available online 25 April 2020

Abbreviations

COPD	chronic obstructive pulmonary disease
TCM	traditional Chinese medicine
BYF	Bufei Yishen formula
ECC	effective-component compatibility
OECC	optimized effective-component compatibility
AECOPD	acute exacerbations of chronic obstructive pulmonary disease
APL	aminophylline
NAC	N-Acetylcysteine
V_T	tidal volume
MV	minute volume
PEF	peak expiratory flow
EF50	expiratory flow at 50% tidal volume
FVC	forced vital capacity
FEV 0.1	forced expiratory volume at 0.1 second
H&E	haematoxylin-eosin
AB-PAS	Alcian Blue/Periodic Acid-Schiff
MLI	alveolar mean linear intercept
MAN	mean alveolar number
BALF	bronchoalveolar lavage fluid
T-AOC	total antioxidant capacity
LPO	lipid peroxidation
IOD	integral optical density
PVDF	polyvinylidene difluoride.

1. Introduction

Chronic obstructive pulmonary disease (COPD), a common, preventable and treatable disease, is mainly manifested as persistent respiratory symptoms and airflow limitation clinically (Patel A R et al., 2019). In China, the prevalence of COPD is 8.6% and the number of patients has reached 100 million that has caused a heavy economic and social burden on the country (Wang C et al., 2018). For thousands of years, traditional Chinese medicine (TCM), including Chinese medicine, acupuncture, and pulmonary rehabilitation has made great contributions to the treatment of COPD, and Chinese herbal formulae are still the most commonly used methods (Ma J et al., 2019; Wang H et al., 2015). In the TCM theory, COPD belongs to the category of lung distention (Feizhang disease) (Tian Y et al., 2016). Lung-kidney Qi deficiency syndrome is one of the most common syndromes of Feizhang disease and the tiaobu Fei-shen therapies are wildly used (Li J, Li Y et al., 2012; Li Y et al., 2014; Gao Z et al., 2018). Bufei Yishen formula (BYF), a representative formula of tiaobu Feishen therapies, with effects of “BuFei YiShen”, “HuaTan” and “HuoXue”, showed beneficial effects on COPD patients by reducing the frequency and duration of acute exacerbations, ameliorating symptoms, and improving exercise endurance and quality of life (Li S et al., 2012). Experimental studies showed that BYF had effects on reducing systemic and pulmonary inflammation, improving protease/anti-protease imbalance and ameliorating collagen deposition on COPD rats (Tian Y et al., 2015; Lu X et al., 2016; Li J et al., 2014; Li J et al., 2015; Tian Y et al., 2017).

BYF is effective, but as a Chinese herbal formula, BYF encounters difficulties in standardization, modernization and internationalization due to its complex composition. Although the exact composition of effective components in herbal medicines is often elusive, it is necessary to explore the effective components and mechanism of them (Jiang Y et al., 2010). In order to identify the bioactive equivalent combinatorial components in BYF, some work has been done. Based on the systems pharmacology, 216 active compounds from BYF and 195 potential targets were found. What's more, the compound-target network showed that herbs acted on similar targets (Li J et al., 2015; Zhao P et al., 2015). After that, we further explored those active components based on inflammatory and/or hypoxic cellular models. 24 components contained in 9 herbal medicines were divided into “BuQi”, “BuShen”, “HuaTan” and “HuoXue” groups to test the effectiveness and to explore the optimal proportion of the components. Finally, we got the effective-component compatibility of BYF I (ECC-BYF I), a combination of 10 compounds, including total ginsenosides, astragaloside IV, icariin, paeonol, etc., and verified its safety and effectiveness on COPD rats.

However, in order to define the optimized bioactive equivalent combinatorial components and to explore the mechanisms, the composition of ECC-BYF I needs to be further optimized. In this work, based on a COPD rat model, we evaluated the efficacy of six optimized effective-component compatibility (OECC) of BYF I-A∼F to elect the optimized formula (ECC-BYF II) by evaluating the changes of lung tissue pathology, pulmonary function, inflammatory response, oxidative stress, and collagen deposition and protease/anti-protease imbalance.

Airway mucus hypersecretion, which manifests clinically as a chronic cough and expectoration, is one of the key characteristics of COPD. Excessive mucus plugs the airways that may cause airflow limitation and provide chances for bacterial infection, which leads to aggravation of the airflow limitation, impaired airway mucociliary transport, respiratory infection and acute exacerbations of COPD (AECOPD) (Zhou-Suckow Z et al., 2017; Shen Y et al., 2018; Tagaya E et al., 2016). We further observed the effects of ECC-BYF II on airway mucus hypersecretion of COPD rats and explored the underlying mechanisms preliminarily. The study results may elucidate the effects of ECC-BYF II on COPD rats and the possible mechanisms on airway mucus hypersecretion.

2. Material and methods

2.1. Animals

Specific pathogen-free Sprague-Dawley rats (200 ± 20 g; 3-months-old) were provided from the Laboratory Animal Center of Henan Province (Zhengzhou, China). The Experimental Animal Care and Ethics Committees in the First Affiliated Hospital, Henan University of Traditional Chinese Medicine (Zhengzhou, China), approved the experimental protocol.

Table 1
The compositions of ECC-BYF I and OECC-BYF I-A∼F.

Formula	Compounds
ECC-BYF I	paeonol, icariin, nobiletin, total ginsenoside, astragaloside IV, peimine, schisandrin B, hesperidin, paeoniflorin, astragalus polysaccharide
OECC-BYF I-A	paeonol, icariin, nobiletin, total ginsenoside, astragaloside IV, peimine, schisandrin B
OECC-BYF I–B	paeonol, icariin, nobiletin, total ginsenoside, astragaloside IV, peimine,
OECC-BYF I–C	paeonol, icariin, nobiletin, total ginsenoside, astragaloside IV, schisandrin B
OECC-BYF I-D	paeonol, icariin, nobiletin, total ginsenoside, peimine, schisandrin B
OECC-BYF I-E	paeonol, icariin, nobiletin, total ginsenoside, astragaloside IV
OECC-BYF I–F	paeonol, icariin, nobiletin, total ginsenoside

2.2. Drugs preparation

Bufei Yishen formula (Patent Number: ZL, 2011 1 0117578.1; Henan medicine: Z20120006) was prepared and provided by the Pharmaceutical Department in Henan University of Chinese Medicine, Zhengzhou, China. The compositions of the formula included Ginseng Radix et Rhizoma (*Panax ginseng C.A. Mey,* 9 g); Astragali Radix (*Astragalus tibetanus Bunge*, 15 g); Corni Fructus (*Cornus officinalis Siebold & Zucc*, 12 g); Lycii Fructus (*Lycium barbarum* L., 12 g); Schisandrae Chinensis Fructus (Schisandra arisanensis Hayata, 9 g); Fritillariae Thunbergii Bulbus (*Fritillaria thunbergii Miq*, 9 g); Perillae Fructus (*Perilla frutescens (L.) Britton*, 9 g); Citri Reticulatae Pericarpium (*Citrus sinensis (L.) Osbeck*, 9 g); Epimedii Folium (*Epimedium acuminatum Franch*, 9 g); Paeoniae Rubra Radix (*Paeonia anomala L*, 9 g); Pheretima (*Pheretima aspergillum (E. Perrier)*,12 g); Ardisiae Japonicae Herba (*Ardisia japonica(Thumb.) Blume*, 15 g). High performance liquid chromatography fingerprint was performed to identify the main chemical constituents in BYF. Fingerprints of BYF and 20 chemical constituents of BYF were identified in previous study (*Zhao P* et al. *J Ethnopharmacol. 2018;217:152-162.*) (Zhao P et al., 2018).

The compositions of ECC-BYF I and OECC-BYF I-A∼F are shown in Table 1. The icariin (MUST-16111710) was purchased from National institutes for food and drug control (Beijing, China). The astragaloside IV (MUST-17022804), schisandrin B (MUST-17031606), peimine (HL-161213), hesperidin (PS170414-09), nobiletin (HL-20170312), paeoniflorin (PS170414-08) and paeonol (MUST-16071405), were obtained from Chengdu Must Bio-Tech Co. Ltd. (Chengdu, China). The astragalus polysaccharide and total ginsenoside were prepared by Dr. Feng suxiang (Henan university of Chinese medicine, China). N-Acetylcysteine tablets (Zambon, Hainan, China; 600mg/tablet) and aminophylline tablets (Xinhua, Shandong, China; 100mg/tablet) were also used.

2.3. COPD model preparation and administration

144 Sprague-Dawley rats were randomized divided into the normal, model, BYF, ECC-BYF I, OECC-BYF I-A∼F, aminophylline (APL) and N-Acetylcysteine (NAC) groups, with equal numbers of males and females in each group. The COPD model was established from week 1 to week 8 using cigarette smoke and bacterial exposure except the normal group (Li Y et al., 2012). The model rats were exposed to tobacco smoke (Hongqiqu® filter cigarettes; Henan Tobacco Industry, Zhengzhou, China) with a smoke density of 3000 ± 500 ppm for 40 min twice daily and the *Klebsiella pneumoniae solution* (6×10^8 CFU/mL, 0.1 mL; ID: 46,114; National Centre for Medical Culture Collection, Beijing, China) was dropped into the nostrils, every 5 days. In the meantime, the normal rats were exposed to fresh air and received 0.1 mL of the saline solution every 5 days.

During week 9 to week 16, the normal and model groups received 2 mL of 0.9% intragastric saline solution twice daily, 6 days/week. BYF (3.7 g/kg/d), ECC-BYF I (9.87 mg/kg), OECC-BYF I-A∼F(6.89 mg/kg/d, 6.35 mg/kg/d, 6.62 mg/kg/d, 6.68 mg/kg/d, 6.07 mg/kg/d, 5.85 mg/kg/d), aminophylline suspension (54 mg/kg/d), and an N-Acetylcysteine suspension (54 mg/kg/d) were given to corresponding groups respectively. Dosages of BYF, aminophylline and N-Acetylcysteine were calculated using the following formula: $D_{rat} = D_{human} \times (K_{rat}/K_{human}) \times (W_{rat}/W_{human})^{2/3}$, where D is the dose, K is the body shape index, and W is the weight. Dosages of ECC-BYF I and OECC-BYF I-A∼F were based on the results of previous experiments. Dosages were recalculated according to weight on Mondays.

2.4. Pulmonary function

The tidal volume (V_T), minute volume (MV), peak expiratory flow (PEF) and expiratory flow at 50% tidal volume (EF50) were detected using unrestrained pulmonary function plethysmography (Buxco Inc. USA) every fourth week from week 0 to week 16. Forced vital capacity (FVC) and forced expiratory volume at 0.1s (FEV 0.1) were measured on the first day of week 17 using a FinePointe™ series PFT system (Buxco Inc. USA).

2.5. Lung and bronchus tissue morphology

Lung tissues and bronchus tissues were cut into 4-mm-thick slices or rings and fixed with 4% paraformaldehyde for 72 h. After conventional dehydration and transparency, the tissues were embedded in paraffin and cut into 4-μm-thick sections. Sections were stained using routine haematoxylin-eosin (H&E) or Alcian Blue/Periodic Acid-Schiff (AB-PAS) processing. Sections were observed and evaluated by optical microscopy and a photographic system (Olympus, Tokyo, Japan). The alveolar mean linear intercept (MLI, μm) and the mean alveolar number (MAN,/mm^2) were counted to assess the degree of emphysema in COPD rats using the counting tool of Adobe Photoshop CC software (Tian Y et al., 2016). The ratio of the AB-PAS-positive staining area to its corresponding bronchial epithelial area was measured by Image Pro Plus 6.0 (IPP 6.0) software to evaluate the rate of goblet cells.

2.6. Analyses of IL-1β, TNF-α, and MUC5AC in the BALF and IL-6, MMP-9, TIMP-1, LPO and T-AOC in the serum

Serum samples from abdominal aorta blood were placed at room temperature for 2 h, followed by centrifugation at 1500 rpm for 15 min. Bronchoalveolar lavage fluid (BALF) was prepared by injecting 3 mL of 4 °C normal saline into the left bronchus for perfusion, followed by pumping back into the centrifuge tube. The operation was repeated 3 times, and then, serum and BALF were collected and stored at −80 °C.

The levels of interleukin (IL)-6, matrix metalloprotein (MMP)-9, and tissue inhibitor of metalloproteinase (TIMP)-1 in the serum and the levels of IL-1β, tumour necrosis factor (TNF)-α, and MUC5AC in the BALF were assayed using enzyme-linked immunosorbent assay (ELISA) according to the manufacturer's introductions (Rat' ELISA Kits for IL-6, IL-1β, TNF-α, MMP-9 and TIMP-1 were provided by Boster Bio-engineering, Wuhan, China. The MUC5AC ELISA Kit was provided by Cloud-Clone Corp, Wuhan, China). Total antioxidant capacity (T-AOC) and lipid peroxidation (LPO) in the serum were detected by a T-AOC kit and an LPO kit (Jiancheng, Nanjing, China).

2.7. Immunohistochemical analysis

The expression of Collagen I and Collagen III in the lung and MUC5AC, MUC5B, EGFR, Akt, and p-mTOR in the airway was tested using immunohistochemistry. Tissue slices were blocked with 3% H_2O_2 for 15 min, and a 5% BSA solution was added. Slices were incubated with an anti-Collagen I antibody (1:50 dilution; Boster Bio-engineering, Wuhan, China), anti-Collagen III antibody (1:1000 dilution; proteintech, Wuhan, China), anti-MUC5AC antibody (1:100 dilution; Elabscience, Wuhan, China), anti-MUC5B antibody (1:200 dilution; Biochemical, Shanghai, China), anti-EGFR antibody (1:100 dilution; GeneTex, CA, USA), anti-AKT antibody (1:500 dilution; GeneTex, CA, USA), anti-p-mTOR antibody (1:500 dilution; GeneTex, CA, USA) overnight at 4 °C. On the next day, slices were incubated with biotin-labelled goat anti-mouse/rabbit immunoglobulin G (ZSGB-BIO, Beijing, China) and stained with a DAB solution (Solarbio, Beijing, China). Six random fields in each section were photographed using an optical microscope and photographic system. The integral optical density (IOD) was counted using IPP 6.0 software.

2.8. Real-time PCR analysis

The expression levels of MUC5AC, MUC5B, EGFR, PI3K, Akt, and mTOR mRNA in the airway were analysed using quantitative real-time PCR (qPCR). The primers were designed and synthesized by Genscript Biotech (Nanjing, China) and are shown in Table 2. Total RNA was

Table 2
Primer sequences of mRNA.

Gene	Primer	Primer Sequence	Length
MUC5AC	Forward primer	CAACACACCACTGCAAGAGC	20
	Reverse primer	GGCTGTGTGGTAGCTGAAGT	20
MUC5B	Forward primer	CCTACGTGCCGCTCTCTAAG	20
	Reverse primer	CAGGCAGGTCAACTTCCCAT	20
EGFR	Forward primer	ACTGCGAGAACCAAGCTACT	20
	Reverse primer	GGAGGCTCAGAAAGTGGTCT	20
PI3K	Forward primer	GAACAGGGCAGCTTCAATGC	20
	Reverse primer	CTCCTTCTGGGTCCGGAGTA	20
Akt	Forward primer	CCTGGACTACTTGCACTCCG	20
	Reverse primer	CACAGCCCGAAGTCCGTTAT	20
mTOR	Forward primer	CTGATGTCATTTATTGGCACAAA	23
	Reverse primer	CAGGGACTCAGAACACAAATGC	22
GAPDH	Forward primer	ACAGCAACAGGGTGGTGGAC	20
	Reverse primer	TTTGAGGGTGCAGCGAACTT	20

extracted using a total RNA extraction kit (Solarbio, Beijing, China) according to the manufacturer's instruction. The Hiscript® II First-Strand cDNA Synthesis Kit (Vazyme, Nanjing, China) was used for the reverse transcription process. The reaction systems were performed using an Applied Biosystems 7500/7500 Fast Real-Time PCR System (AB, Foster City, United States). The process of initial enzyme activation was set at 95 °C for 5 min, followed by 40 cycles of 95 °C for 10 s and 60 °C for 30 s. The melting curve range was set as 95 °C for 15 s, 60 °C for 60 s and 95 °C for 15 s.

2.9. Western blotting

The protein expression levels of EGFR, PI3K, Akt, mTOR, phosphorylated EGFR (p-EGFR), phosphorylated PI3K (p-PI3K), phosphorylated Akt (p-Akt), and phosphorylated mTOR (p-mTOR) in the airway were measured using western blotting. After total protein collection by a protein extraction kit (Solarbio, Beijing, China), the BCA

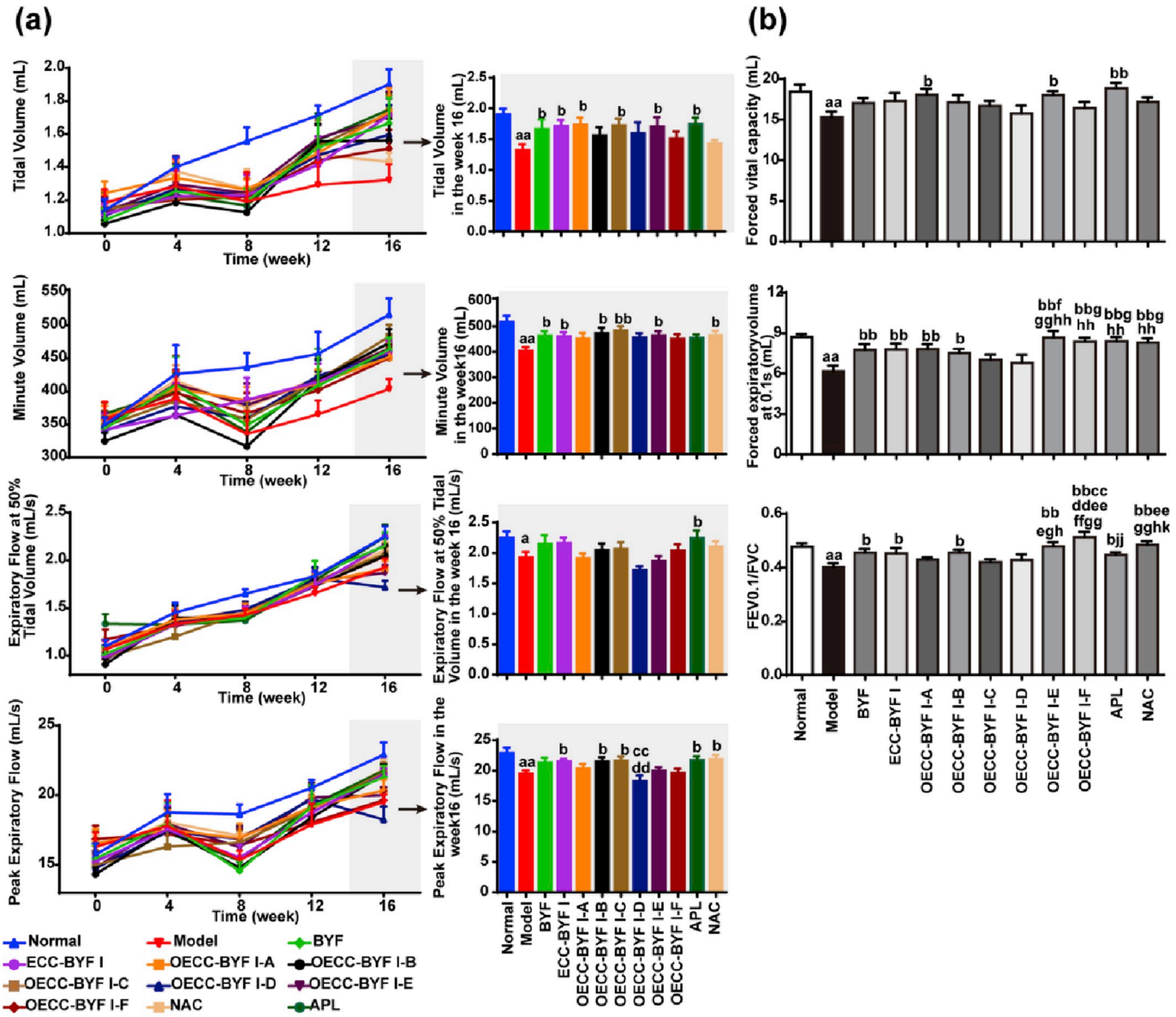

Fig. 1. Changes of the pulmonary function in all groups. (a) Changes of V_T, MV, EF50 and PEF in all groups. **(b)** Changes of FVC, FEV0.1 and FEV0.1/FVC in all groups. The data are expressed as the means ± SE, (n = 8–12). $^{a}P < 0.05$ vs. the normal group, $^{aa}P < 0.01$ vs. the normal group; $^{b}P < 0.05$ vs. the model group, $^{bb}P < 0.01$ vs. the model group; $^{cc}P < 0.01$ vs. the BYF group; $^{dd}P < 0.01$ vs. the ECC-BYF I group; $^{e}P < 0.05$ vs. the OECC-BYF I-A group, $^{ee}P < 0.01$ vs. the OECC-BYF I-A group; $^{f}P < 0.05$ vs. the OECC-BYF I–B group, $^{ff}P < 0.01$ vs. the OECC-BYF I–B group; $^{g}P < 0.05$ vs. the OECC-BYF I–C group, $^{gg}P < 0.01$ vs. the OECC-BYF I–C group; $^{h}P < 0.05$ vs. the OECC-BYF I-D group, $^{hh}P < 0.01$ vs. the OECC-BYF I-D group; $^{jj}P < 0.01$ vs. the OECC-BYF I–F group; $^{k}P < 0.05$ vs. the APL group.

protein assay kit (Solarbio, Beijing, China) was used to detect the concentrations of protein. Denatured protein (40 μg) was separated using electrophoresis and transferred to polyvinylidene difluoride (PVDF) membranes (Millipore, Bedford, USA). Membranes were blocked with 5% non-fat dry milk, and incubated with the following primary antibodies (GeneTex, CA, USA): anti-EGFR (1:1000 dilution), p-EGFR (1:500 dilution), PI3K (1:1500 dilution), p-PI3K (1:750 dilution), Akt (1:5000 dilution), p-Akt (1:2000 dilution), mTOR (1:1000 dilution), p-mTOR (1:1000 dilution) and GAPDH (1:5000 dilution; Proteintech, Wuhan, China). The signals were visualized using the Super ECL Plus reagent (Solarbio, Beijing, China) and measured by the Chemi DocTM MP System (Bio-Rad, CA, USA).

2.10. Statistical analysis

Data were analysed using IBM SPSS 22.0 software and the results are expressed as the mean ± standard error (SE). one-way analysis of variance (ANOVA) was employed for multiple comparisons. The significance level was set as $P < 0.05$.

2.11. R-value comprehensive evaluation

To evaluate the comprehensive effects of the drugs (BYF, ECC-BYF I, OECC-BYF I-Ã F, APL and NAC), the R-value comprehensive evaluation was used. Firstly, we evaluated the comprehensive outcome which

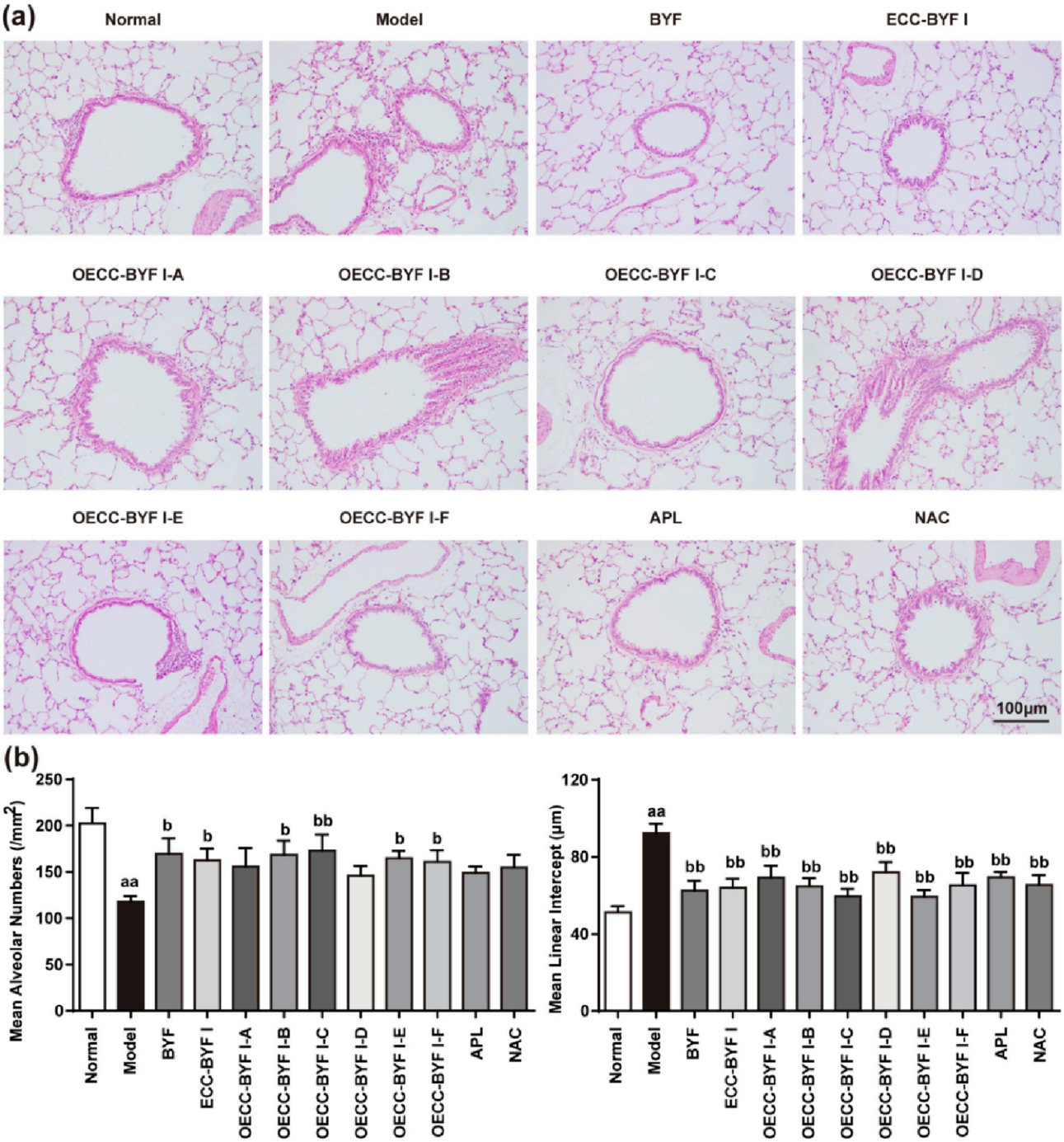

Fig. 2. Pathological changes in the lung tissues in all groups. **(a)** Photograph of lung tissue pathology (HE, 200 ×); **(b)** Changes of MAN and MLI. The values are expressed as the means ± SE, ($n = 6$). $^{aa}P < 0.01$ vs. the normal group; $^{b}P < 0.05$ vs. the model group, $^{bb}P < 0.01$ vs. the model group.

contains 19 indicators (pulmonary function: V_T, MV, PEF, EF50, FVC, FEV 0.1, FEV 0.1/FVC; histological changes: MLI, MAN; IL-1β, IL-6, TNF-α, MMP-9, TIMP-1, T-AOC, LPO, MUC5AC, Collagen I and Collagen III). Secondly, we evaluated the effects of the drugs from different perspectives on pulmonary function (V_T, MV, PEF, EF50, FVC, FEV 0.1 and FEV 0.1/FVC); inflammation and oxidative stress (IL-1β, IL-6, TNF-α, T-AOC and LPO); protease/anti-protease imbalance and collagen deposition (MMP-9, TIMP-1, Collagen I and Collagen III).

The R-value of the outcomes is calculated to evaluate comprehensive effects of the drugs. $\bar{x}$ and s represent the mean value and standard deviation of the outcomes (lung function: V_T, MV, PEF, EF50, FVC, FEV 0.1, FEV 0.1/FVC; histological changes: MLI, MAN; IL-1β, IL-6, TNF-α,

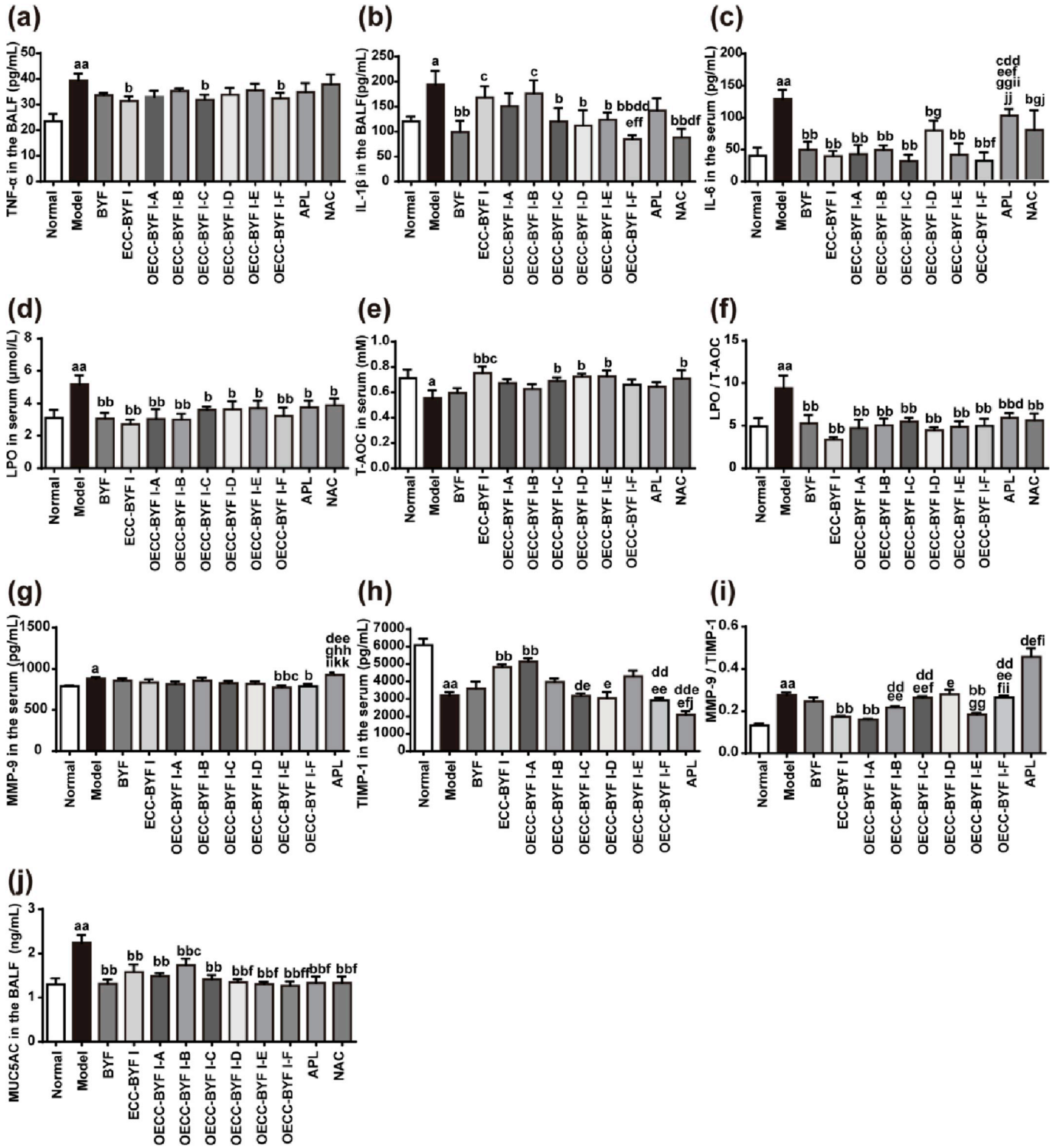

Fig. 3. Changes of TNF-α, IL-1β, MUC5AC in the BALF and IL-6, LPO, T-AOC, LPO/T-AOC, MMP-9, TIMP-1 and MMP-9/TIMP-1 in the serum in all groups. The values are expressed as the means ± SE, (n=6). $^{a}P < 0.05$ vs. the normal group, $^{aa}P < 0.01$ vs. the normal group; $^{b}P < 0.05$ vs. the model group, $^{bb}P < 0.01$ vs. the model group; $^{c}P < 0.05$ vs. the BYF group; $^{d}P < 0.05$ vs. the ECC-BYF I group, $^{dd}P < 0.01$ vs. the ECC-BYF I group; $^{e}P < 0.05$ vs. the OECC-BYF I-A group, $^{ee}P < 0.01$ vs. the OECC-BYF I-A group; $^{f}P < 0.05$ vs. the OECC-BYF I-B group, $^{ff}P < 0.01$ vs. the OECC-BYF I-B group; $^{g}P < 0.05$ vs. the OECC-BYF I-C group, $^{gg}P < 0.01$ vs. the OECC-BYF I-C group; $^{ii}P < 0.01$ vs. the OECC-BYF I-E group; $^{j}P < 0.05$ vs. the OECC-BYF I-F group, $^{jj}P < 0.01$ vs. the OECC-BYF I-F group.

MMP-9, TIMP-1, T-AOC, LPO, MUC5AC, Collagen I and Collagen III), respectively. The groups are represented as: Normal group $\bar{x}_1 \pm s_1$, Model group $\bar{x}_2 \pm s_2$, BYF group $\bar{x}_3 \pm s_3$, ECC-BYF I group $\bar{x}_4 \pm s_4$, OECC-BYF I-A group $\bar{x}_5 \pm s_5$, OECC-BYF I–B group $\bar{x}_6 \pm s_6$, OECC-BYF I–C group $\bar{x}_7 \pm s_7$, OECC-BYF I-D group $\bar{x}_8 \pm s_8$, OECC-BYF I-E group $\bar{x}_9 \pm s_9$, OECC-BYF I–F group $\bar{x}_{10} \pm s_{10}$, APL group $\bar{x}_{11} \pm s_{11}$, and NAC group $\bar{x}_{12} \pm s_{12}$.

The R-value is calculated according to formulas (1) ~ (5).

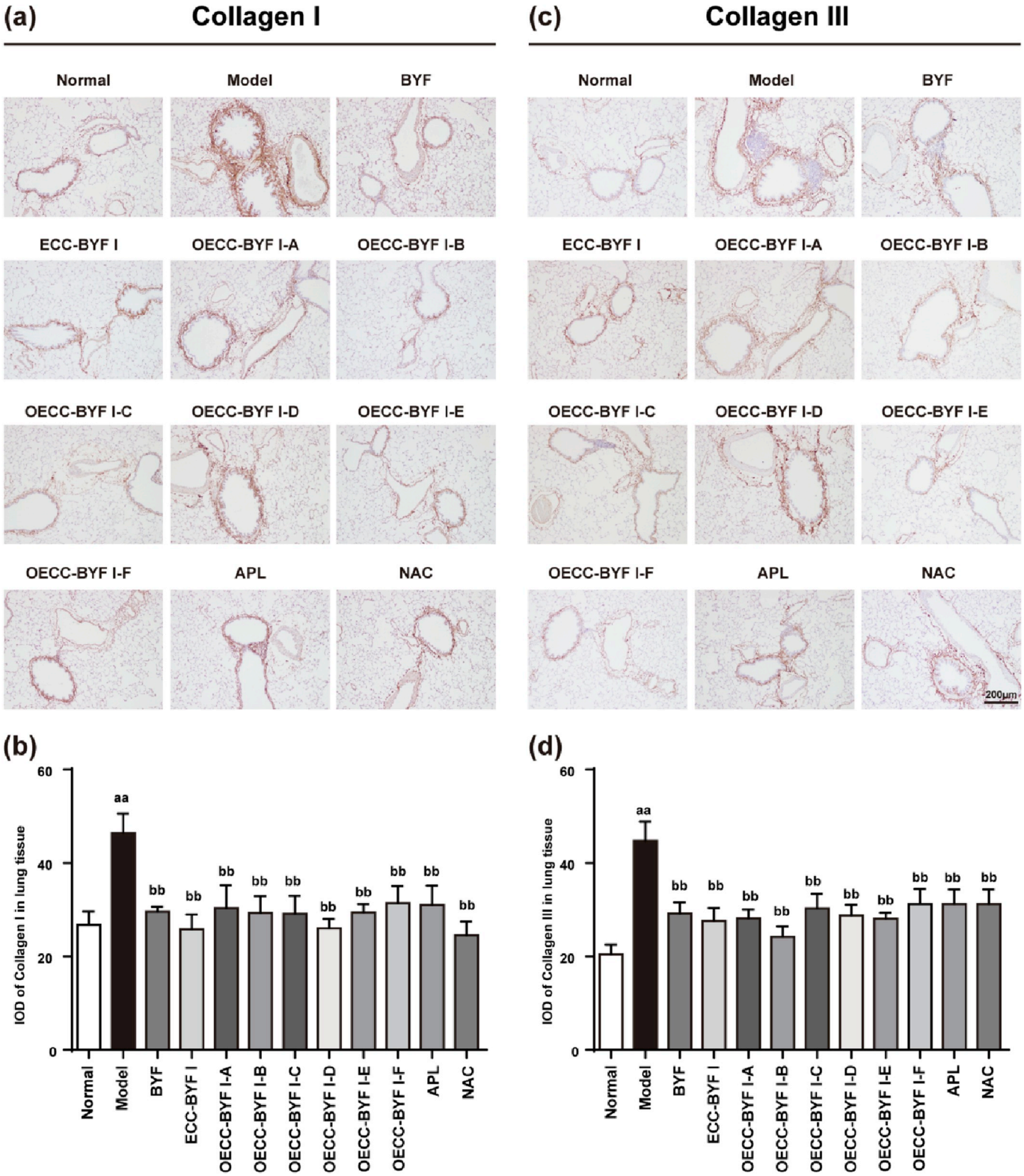

Fig. 4. Changes of Collagen I and Collagen III in the lung tissue in all groups. (a) and (c): Changes of Collagen I and Collagen III in the lung tissue (IHC, 100 ×); **(b) and (d):** Changes of IODs of Collagen I and Collagen III in all groups. The values are expressed as the means ± SE, (n = 6). $^{aa}P < 0.01$ vs. the normal group; $^{bb}P < 0.01$ vs. the model group.

Formula of

$$\text{model effect: } dM = \frac{\bar{x}_2 - \bar{x}_1}{z_1} \qquad s = \frac{s_2 + s_1}{2} \tag{1}$$

Formula of treatment effects (Take BYF and ECC-BYF I for examples):

$$\text{BYF effect} \quad dMe_1 = \frac{\bar{x}_3 - \bar{x}_2}{z_1} \qquad z_1 = \frac{s_2 + s_3}{2}; \tag{2}$$

$$\text{ECC} - \text{BYF I effect} \quad dMe_2 = \frac{\bar{x}_4 - \bar{x}_2}{z_1} \qquad z_2 = \frac{s_2 + s_4}{2}; \tag{3}$$

$$\text{R- value } R_i = \frac{dMe_i}{dM}, \ i = 1, \ldots\ldots, 11. \tag{4}$$

For convenience of calculations, we transformed the R-values to D-values.

$$D = R - (-1) \tag{5}$$

The data sets underwent test of normality and homogeneity of variances. Least significant deviation (LSD) of one-way ANOVA was used in the data meeting normal distributions, while Dunnett's T3 was used in other data. The α level of significance was set at 0.05. Values were expressed as means ± standard errors.

3. Result

3.1. Therapeutic effects of OECC-BYF I on COPD rats

3.1.1. OECC-BYF I improved pulmonary function and pathological changes of COPD rats

To observe the effects of BYF, ECC-BYF I and OECC-BYF I on COPD rats induced by cigarette smoke combined with *Klebsiella pneumoniae*, unrestrained pulmonary function plethysmography was used to detect V_T, MV, PEF and EF50 every fourth week, and the PFT system was used to measure the FVC and FEV 0.1 after 8 weeks of administration. Fig. 1 shows significantly decreased pulmonary function in the COPD rats, indicating airflow limitation in the model rats. After 8 weeks of treatment, BYF, ECC of BYF I, and OECC of BYF I effectively improved the ventilatory function of COPD rats. Compared with the positive control drug aminophylline, there was no significant difference between the effects of APL and OECC of BYF I.

The pathological features of COPD are mainly manifest as an expansion of the alveolar cavity and inflammatory cell infiltration in the lung. The present study observed lung histopathological changes in

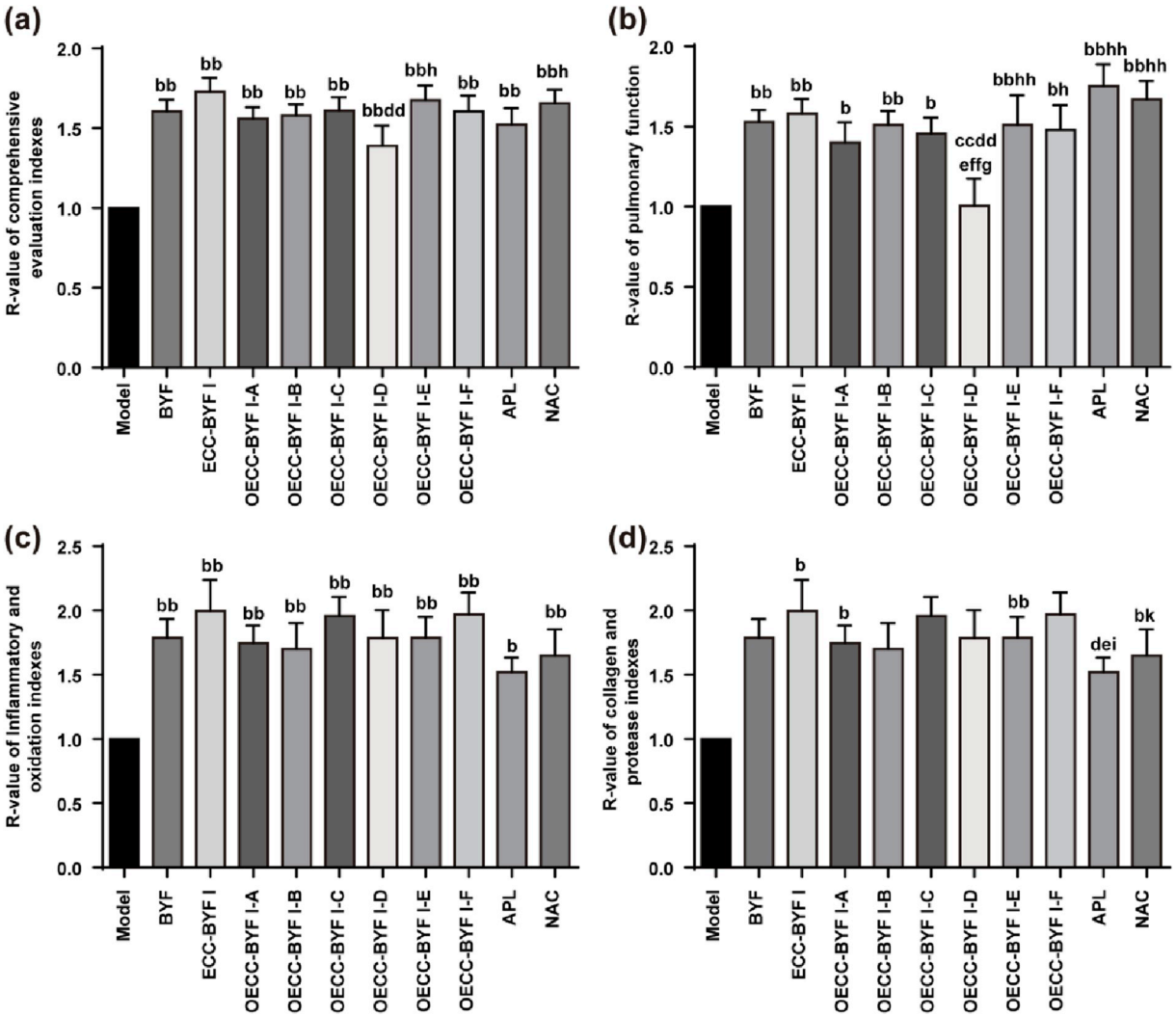

Fig. 5. Changes of R-Value in all groups. **(a)**: The R-Value of comprehensive evaluation indexes (n = 19). **(b)**: The R-Value of pulmonary function (n = 7). **(c):** The R-Value of IL-1β、IL-6、TNF-α、LPO and T-AOC (n = 5). **(d):** The R-Value of MMP-9、TIMP-1、Collagen I and Collagen III (n = 4). The values are expressed as the means ± SE. $^{b}P < 0.05$ vs. the model group, $^{bb}P < 0.01$ vs. the model group; $^{cc}P < 0.01$ vs. the BYF group; $^{d}P < 0.05$ vs. the ECC-BYF I group, $^{dd}P < 0.01$ vs. the ECC-BYF I group; $^{e}P < 0.05$ vs. the OECC-BYF I-A group; $^{ff}P < 0.01$ vs. the OECC-BYF I–B group; $^{g}P < 0.05$ vs. the OECC-BYF I–C group; $^{h}P < 0.05$ vs. the OECC-BYF I-D group, $^{hh}P < 0.01$ vs. the OECC-BYF I-D group; $^{i}P < 0.05$ vs. the OECC-BYF I-E group; $^{k}P < 0.05$ vs. the APL group.

COPD rats (Fig. 2). The structure of bronchioles and alveoli in the normal rats was complete, and few inflammatory cells were observed. Lung tissues in the model group showed obvious alveolar fracture and fusion as well as airspace enlargement. Lots of inflammatory cells were observed in the bronchiole and alveolar space. The treatment groups showed improvement: the alveolar structure was basically normal, with less inflammatory exudates. In improving the histopathological damage, there is no significant difference among the BYF, ECC-BYF I and OECC-BYF I-A∼F groups.

3.1.2. OECC-BYF I reduced inflammation and oxidative stress in COPD rats

Chronic respiratory inflammation is one characteristic of COPD. To observe the inhibition effects of BYF, ECC-BYF I and OECC-BYF I on the inflammation of COPD rats, ELISA was used to detect the levels of representative inflammatory factors (IL-6, IL-1β and TNF-α). The present study showed that the BYF, ECC-BYF I, OECC-BYF I-A∼F, and NAC reduced the high levels of IL-6 in the serum. The OECC-BYF I-A, OECC-BYF I–C and OECC-BYF I-E, reduced the level of TNF-α, and the BYF, OECC-BYF I–C, -D, -E, –F and NAC reduced the level of IL-1β in the BALF of COPD rats (Fig. 3a–c), which indicated that the BYF, ECC-BYF I and OECC-BYF I inhibited the local inflammation in the lung and the systemic inflammatory response of COPD.

Since oxidative stress plays an important role in the pathogenesis of COPD and there are oxidative stress biomarkers in the airway, sputum and blood, we tested the levels of LPO and T-AOC in COPD rats and found that the levels were significantly changed. Each treatment reduced the level of LPO. By improving the T-AOC indicator, the ECC-BYF I, OECC-BYF I–C, -D, -E, and NAC groups showed better effects (Fig. 3d–f).

3.1.3. OECC-BYF I improved collagen deposition and protease/anti-protease imbalance and reduced airway mucus in COPD rats

Matrix metalloproteinases (MMPs), together with their inhibitors, tissue inhibitor of metalloproteinases (TIMPs), affect the homeostasis of elastin and collagen, which are important for the structural integrity of human airways. MMP-9 and TIMP-1 are closely related to COPD airway remodeling and were tested in this study. We found that in COPD rats, the ratio of MMP-9/TIMP-1 increased significantly, and ECC-BYF I,

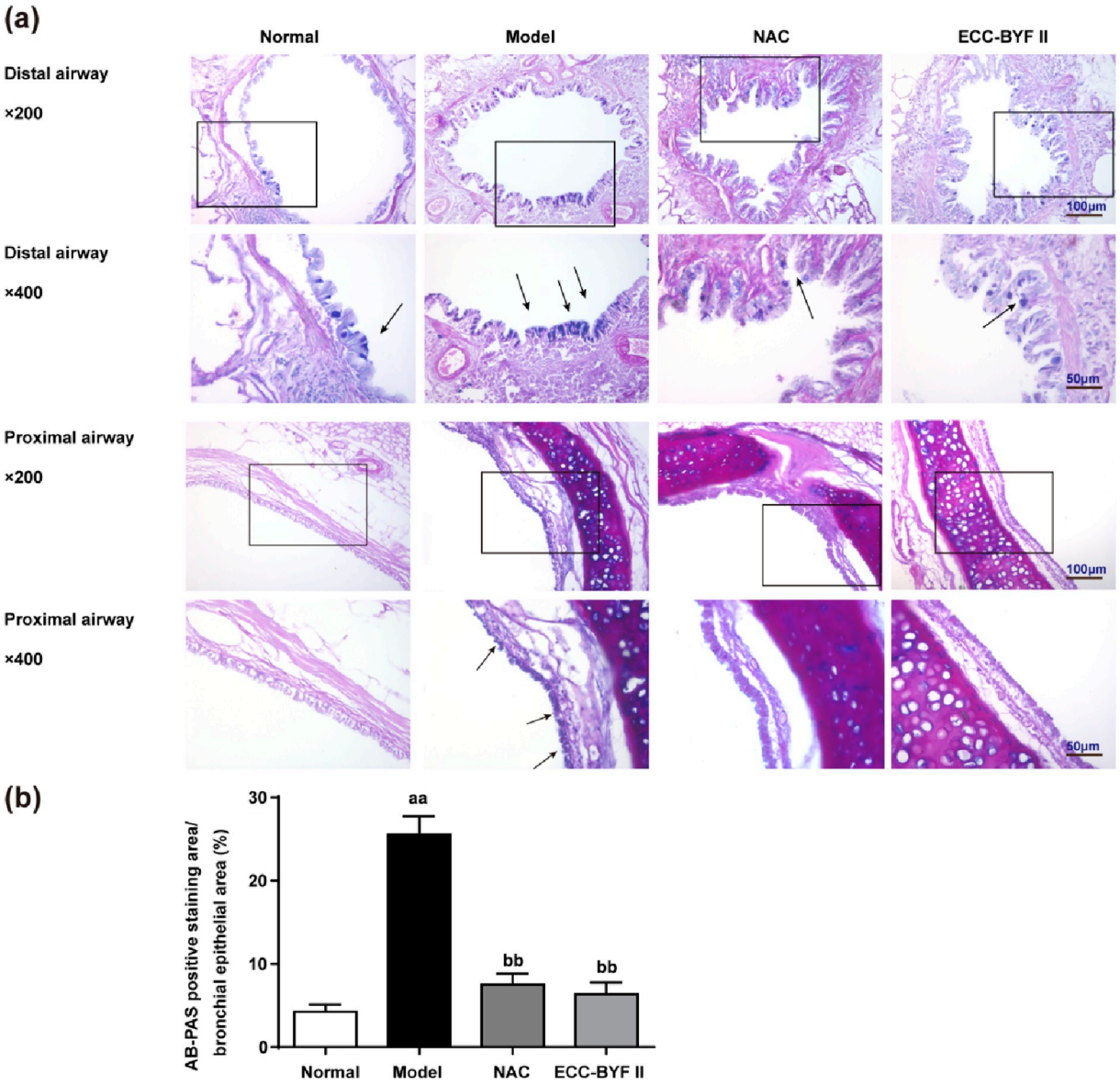

Fig. 6. Changes in goblet cells in the airway. (a): AB-PAS staining photos of the proximal airway and distal airway in all groups (AB-PAS; 200 × , 400 ×). →: goblet cell. (b): The ratio of AB-PAS-positive staining area to its corresponding bronchial epithelial area (%). The data are expressed as the mean ± SE (n = 6). $^{aa}P < 0.01$ vs. the normal group; $^{bb}P < 0.01$ vs. the model group.

OECC-BYF I-A and OECC-BYF I-E effectively improved the imbalance of MMP-9/TIMP-1 (Fig. 3g–i).

Cigarette smoke and other irritants cause inflammatory reactions and oxidative stress, which induce damage to airway epithelial cells and stimulate mucus hypersecretion. MUC5AC, a representative indicator of airway mucus hypersecretion, was detected by ELISA. The results of this study showed that the high level of MUC5AC in the BALF in COPD rats was reduced by treatment with BYF, ECC-BYF I, OECC-BYF I-A∼F, APL and NAC (Fig. 3j).

Persistent inflammation and oxidative stress caused by repeated cigarette smoke stimulation also lead to the remodeling of the lung parenchyma and airways. The expression levels of extracellular matrix protein including collagen I and collagen III were detected. As shown in Fig. 4, the expression levels of collagen I and collagen III in the lung tissues of COPD rats were markedly decreased after the administrations of BYF, ECC-BYF I, OECC-BYF I-A∼F, APL and NAC.

3.1.4. R-value comprehensive evaluation showed that OECC-BYF I had beneficial effect on COPD rats and OECC-BYF I-E was the optimal formula

The results of R-value comprehensive evaluation showed that all the treatments had therapeutic effect on COPD rats. Compared with BYF and ECC-BYF I, OECC-BYF I-A, OECC-BYF I–B, OECC-BYF I–C, OECC-BYF I-E and OECC-BYF I–F showed no significant difference. OECC-BYF I-E was the optimal formula which was named ECC-BYF II (Fig. 5a).

We further analysed the results and found that there were different efficacy characteristics of the treatments. In improving pulmonary function, APL had advantages, followed by NAC, ECC-BYF I, BYF, OECC-BYF I–B and OECC-BYF I-E (Fig. 5b). ECC-BYF I, OECC-BYF I–F, OECC-BYF I–C, BYF and OECC-BYF I-D had advantages in inhibiting inflammation and oxidative stress (Fig. 5c). In improving protease/anti-protease imbalance and collagen deposition, ECC-BYF I, OECC-BYF I-A, OECC-BYF I-E and NAC groups had improvement compared with the COPD rats (Fig. 5d).

3.2. ECC-BYF II inhibits mucus hypersecretion of COPD rats by regulating the EGFR/PI3K/mTOR pathway

To explore the effect of ECC-BYF II on COPD mucus hypersecretion, airway pathological changes and airway mucin expression were observed. Excessive hyperplasia of goblet cells and hypertrophy of airway submucosal glands are the pathological bases of mucus hypersecretion in COPD. As shown in Fig. 6, AB-PAS staining showed few blue-stained goblet cells in the airway epithelium in normal rats, and many blue-stained goblet cells were observed in COPD rats. Data showed that ECC-BYF II had positive effects on reducing goblet cell metaplasia and airway remodeling induced by cigarette smoke and bacterial exposure.

MUC5AC and MUC5B are the dominant components of airway mucus that were detected in this study by immunohistochemistry and qPCR. As shown in Fig. 7, MUC5AC was primarily expressed in the airway epithelium, and MUC5B was primarily expressed in the submucosa of bronchial and bronchioles. The protein and mRNA expression levels of MUC5AC and MUC5B increased markedly in COPD rats and were obviously downregulated by ECC-BYF II and NAC, as were MUC5AC levels in the BALF. There was no difference between ECC-BYF II and NAC in reducing the levels of airway mucus.

3.3. ECC-BYF II regulated the EGFR/PI3K/mTOR pathway

The EGFR signaling network has significant effects on the regulation of mucus hypersecretion via the activation of multiple downstream pathways to stimulate goblet cell proliferation (He M et al., 2018). To further examine the underlying effects of ECC-BYF II on COPD mucus

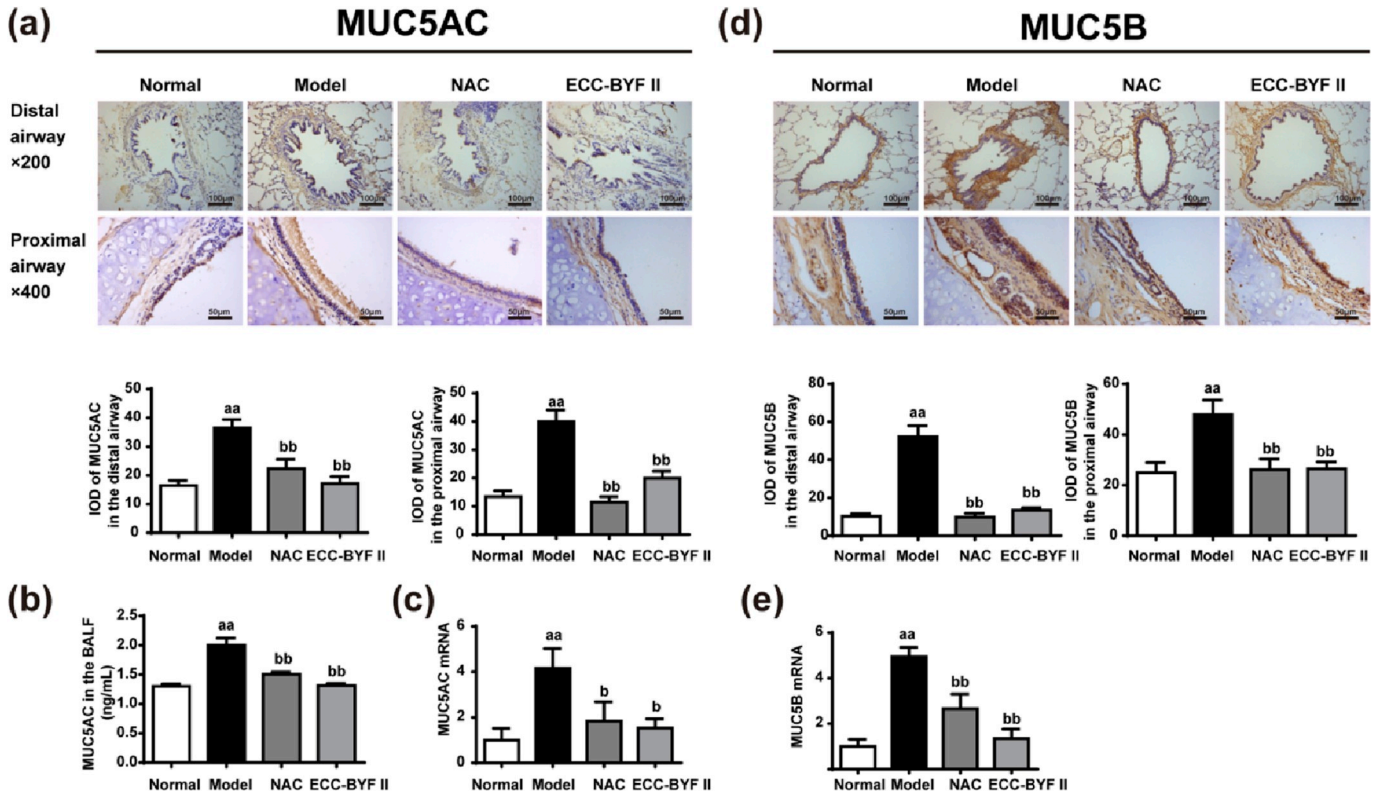

Fig. 7. Expression levels of MUC5AC, MUC5B in the airway and the levels of MUC5AC in the BALF. (a): The expression level of MUC5AC in the proximal airway and distal airway tested using immunohistochemistry (200 × , 400 ×); (b): The level of MUC5AC in the BALF (ng/mL); (c): The mRNA expression level of MUC5AC. Values are the mean ± SE, (n = 6). (d): The expression level of MUC5B in the proximal airway and distal airway tested using immunohistochemistry (200 × , 400 ×); (e): The mRNA expression level of MUC5B. Values are the mean ± SE, (n = 6). $^{aa}P < 0.01$ vs. the normal group; $^{b}P < 0.05$ vs. the model group, $^{bb}P < 0.01$ vs. the model group.

hypersecretion, we next detected activated proteins related to the EGFR/PI3K/mTOR pathway.

The immunohistochemical results showed increased expression levels of EGFR, Akt and p-mTOR in COPD rats compared to those in normal rats. The expression levels of EGFR, Akt, and p-mTOR in the airways were decreased after ECC-BYF II administration (Fig. 8). As shown in Fig. 9, the mRNA, protein and phosphorylated protein expression levels of EGFR, PI3K, Akt, and mTOR in the airways of COPD rats were increased compared to those in the normal group, and significantly reduced in ECC-BYF II group. The above results suggested that the protein and mRNA expression levels of EGFR, PI3K, Akt, and mTOR were upregulated in COPD rats and downregulated after the administration of ECC-BYF II.

4. Discussion

Traditional Chinese medicine has shown effectiveness and safety in COPD treatment. BYF, a traditional herbal formula for COPD composed of 12 medicinal herbs was made from highly concentrated, selected Chinese herbs and was produced in accordance with the traditional Chinese formula. BYF was constructed by professor Jiansheng Li; according to TCM theory, BYF has the effects of “BuFei YiShen”, “HuaTan” and “HuoXue”, which are suitable for the COPD pathogenesis of deficiency of lung and kidney qi. In a previous clinical study, a four-center, open-label, randomized, controlled study confirmed that BYF had beneficial effects on stable COPD patients by alleviating the clinical symptoms (Li J, Li S Y et al., 2012).

However, as an herbal formula, BYF presents difficulties in standardizing its composition and clarifying the mechanisms due to its complex, multi-component composition. Efforts have been made to explore the active ingredients of BYF. In previous research, systematic pharmacology revealed the active compounds and potential targets of BYF (Li J et al., 2015). In vitro experiments based on an orthogonal design, we further explored the effectiveness and optimized the

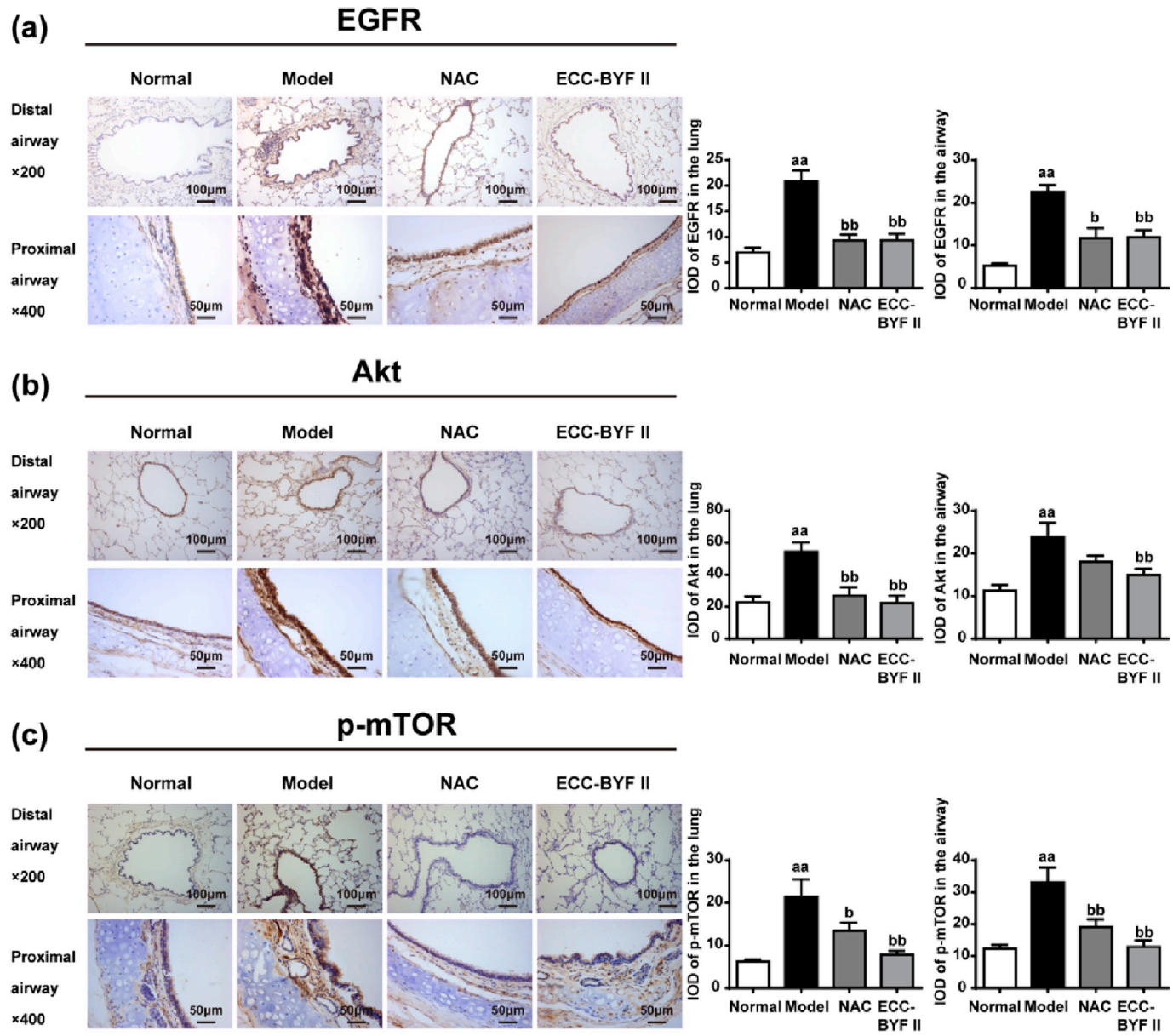

Fig. 8. Expression levels of EGFR, Akt and p-mTOR in the airways in all groups. (a): The expression of EGFR in the airway tested using immunohistochemistry (200 × , 400 ×); (b): The expression of Akt in the airway tested using immunohistochemistry (200 × , 400 ×); (c): The expression of p-mTOR in the airway tested using immunohistochemistry (200 × , 400 ×). Values are the mean ± SE, (n = 6). $^{aa}P < 0.01$ vs. the normal group; $^{b}P < 0.05$ vs. the model group, $^{bb}P < 0.01$ vs. the model group.

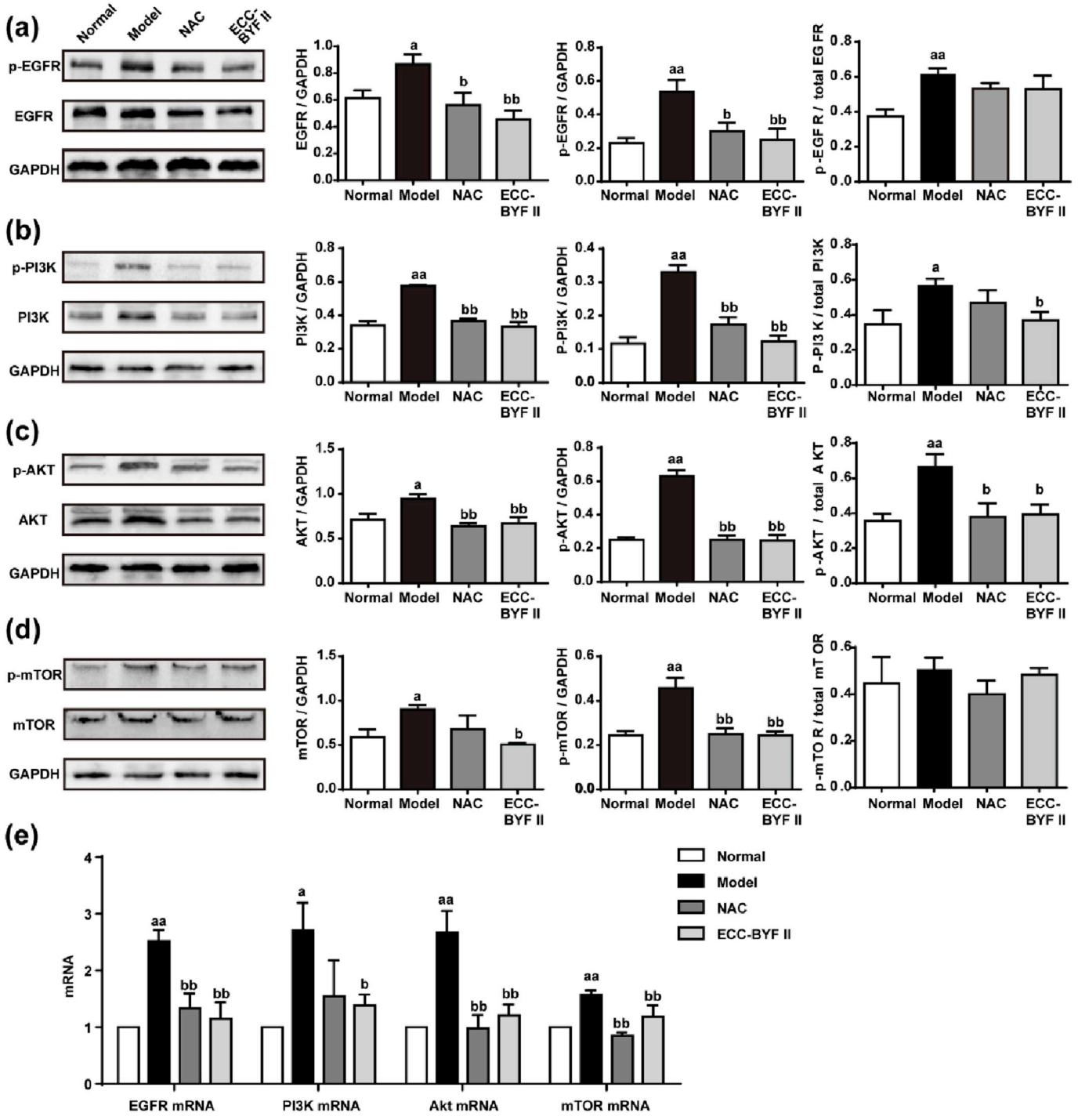

Fig. 9. Protein and mRNA expression levels of EGFR, PI3K, Akt, and mTOR in the airway of COPD rats. (a–d): The protein expression levels of p-EGFR, EGFR, p-PI3K, PI3K, p-Akt, Akt, p-mTOR and mTOR. Values are the mean ± SE, (n = 3) (e): The mRNA expression levels of EGFR, PI3K, Akt, and mTOR in the airway. Values are the mean ± SE, (n = 6). $^{a}P < 0.05$ vs. the normal group, $^{aa}P < 0.01$ vs. the normal group; $^{b}P < 0.05$ vs. the model group, $^{bb}P < 0.01$ vs. the model group.

proportions of the components and obtained ECC-BYF I. The effects and dosage of ECC-BYF I were tested on a COPD rat model.

In this study, to further simplify the composition of ECC-BYF I, seven components (paeonol, icariin, nobiletin, total ginsenoside, astragaloside IV, peimine and schisandrin B) that showed stronger effects in previous cellular experiments were selected. These seven components have different effects in Chinese medicine theory. Total ginsenoside and astragaloside IV have “BuQi” effects; icariin and schisandrin B have “BuShen” effects; nobiletin and peimine have “HuaTan” effects; and paeonol has a “HuoXue” effect. Based on the Chinese medicine compatibility theory, these seven components were combined into six groups: optimized ECC-BYF I-A∼F.

We further tested the effects of ECC-BYF I-A∼F based on the efficacy of drugs in several aspects, which are closely related to the pathogenesis or pathology of COPD. Changes in lung tissue pathology, pulmonary function, inflammatory response, oxidative stress, collagen deposition and protease/anti-protease imbalance, and airway mucus were evaluated. With equal efficacy, we optimized ECC-BYF I with 10 components (paeonol, icariin, nobiletin, total ginsenoside, astragaloside IV, peimine, schisandrin B, hesperidin, paeoniflorin, astragalus

polysaccharide) to OECC-BYF I-E (ECC-BYF II) with components of 5 ingredients (paeonol, icariin, nobiletin, total ginsenoside, astragaloside IV).

ECC-BYF II has shown beneficial efficacy in COPD rats for improving pulmonary function and lung tissue pathological damage, reducing systemic and local inflammatory responses, and alleviating oxidative stress and collagen deposition. Finally, based on BYF, an effective Chinese herbal formula for the treatment of COPD consisting of twelve medicinal herbs, we obtained ECC-BYF II. The results showed that ECC-BYF II, a formula composed of five kinds of standard components, has equivalent efficacy to BYF and ECC-BYF I. ECC-BYF II has the advantages that it is guided by the theory and principle of holistic concepts and pattern differentiation in TCM and is characterized by its standard components.

COPD is a major cause of morbidity and mortality globally; airway mucus hypersecretion is one of its key characteristics (Ramos F L et al., 2014; Choi W et al., 2020). Airway mucus hypersecretion, together with impaired mucus clearance function, cause airway airflow limitations and infection, which contribute to the decreased pulmonary function and AECOPD (Whitsett J A 2018). The current study demonstrated that mucus hypersecretion was an independent risk factor for COPD and that it was related to disease progression and poor prognosis. MUC5AC and MUC5B are secreted gel-forming mucins that dominate the biophysical properties of airway mucus (Livraghi-Butrico A et al., 2017; Okuda K et al., 2019). These proteins play important roles in chronic bronchitis pathophysiology, and their expression negatively correlates with the pulmonary function of COPD patients (Kesimer M et al., 2017; Liu W et al., 2020).

Airway mucins are produced by goblet cells and airway submucosal glands, which are regulated by multiple signaling pathways; the most important pathway is the EGFR pathway. EGFR activates multiple downstream pathways, such as the PI3/Akt and nuclear factor kappa B (NF-κB) pathways, to promote goblet cell hyperplasia (GCH) and the hypersecretion of airway mucus (Song W Y et al., 2017; Jia Z et al., 2020; Wang J et al., 2019). PI3K/Akt is a vital downstream pathway of the EGF receptor family. Activated EGFR combines with the adaptor protein Gab1, and Gab1 is phosphorylated and abundantly recruits the downstream protein PI3K. The main product of PI3K, phosphatidylinositol-3,4,5-triphosphate (PIP3), is a surface receptor for a variety of cells and may associate with Akt (Wang J et al., 2020). After Akt activation, phosphorylation of tuberous sclerosis-associated proteins 2 and 1 (TSC2, TSC1) leads to their inactivation, which leads to the activation of rapamycin (mTOR). Several downstream proteins are activated by mTOR, followed by increased expression of mucins (Sheaffer K L et al., 2008; Ganesan S and Sajjan U S 2013). Recent research reported that the downregulation of the EGFR/PI3K/Akt pathway inhibited mucus hypersecretion in COPD (Feng F et al., 2019).

We next observed the effects of ECC-BYF II on airway mucus hypersecretion in COPD rats and explored the underlying mechanisms of the EGFR/PI3K/mTOR pathway. Changes in airway pathology, expression levels of MUC5AC and MUC5B and changes in goblet cells were observed to evaluate the effect of ECC-BYF II on controlling airway mucus hypersecretion. NAC exhibits a positive effect on mucus dissolution; therefore, it was used as the positive control drug (Kalyuzhin O V 2018). The results confirmed that ECC-BYF II significantly reduced airway mucus hypersecretion, and the effects of ECC-BYF II on inhibiting goblet cell hyperplasia and reducing MUC5AC and MUC5B over-expression showed no difference from NAC. The results also suggested that the potential mechanism by which ECC-BYF II inhibits mucus hypersecretion may be related to the regulation of the EGFR/PI3K/mTOR pathway. However, there may be other mechanisms by which ECC-BYF II affects the secretion of airway mucus. We will attempt to clarify the mechanisms of ECC-BYF II in future research.

In conclusion, ECC-BYF II, which consists of five standard components (paeonol, icariin, nobiletin, total ginsenoside, astragaloside IV), has equivalent efficacy to BYF and ECC-BYF I in COPD rats. ECC-BYF II has beneficial effects in COPD rats by improving the pulmonary function, reducing the lung tissue pathological damage and inflammatory responses, and alleviating oxidative stress and collagen deposition. We also confirmed that ECC-BYF II effectively reduced airway mucus hypersecretion in COPD rats. The potential mechanism by which ECC-BYF II inhibits the airway mucus hypersecretion of COPD may be related to the regulation of the EGFR/PI3K/mTOR pathway. The mechanism still needs to be demonstrated through further research.

Author contributions

L JS, T YG, Z P contributed to the study design. M JD performed the experiments performing, data analysis and manuscript drafting. F SX contributed to the BYF preparation. L XF, D HR, Z WC, Z LX, W MM, Z LH, L S and Z D performed the animal experiments and pulmonary function testing. M JD and L JS contributed to this work equally. All the authors had read and approved the final version of the manuscript.

Funding

The research is supported by National Natural Science Foundation of China (No. 81973822, 81130062).

Acknowledgments

There are no known conflicts of interest associated with this publication and there has been no significant financial support for this work that could have influenced its outcome.

The datasets used to support the findings of this study are available from the corresponding author upon request.

Appendix A. Supplementary data

Supplementary data to this article can be found online at https://doi.org/10.1016/j.jep.2020.112796.

References

Choi, W., Choe, S., Lin, J., et al., 2020. Exendin-4 restores airway mucus homeostasis through the GLP1R-PKA-PPARgamma-FOXA2-phosphatase signaling. Mucosal Immunol. https://doi.org/10.1038/s41385-020-0262-1.

Feng, F., Du, J., Meng, Y., et al., 2019. Louqin zhisou decoction inhibits mucus hypersecretion for acute exacerbation of chronic obstructive pulmonary disease rats by suppressing EGFR-PI3K-AKT signaling pathway and restoring Th17/Treg balance. Evid. base Compl. Alternative Med., 6471815. https://doi.org/10.1155/2019/6471815. 2019.

Ganesan, S., Sajjan, U.S., 2013. Repair and remodeling of airway epithelium after injury in chronic obstructive pulmonary disease. Curr Respir Care Rep 2. https://doi.org/10.1007/s13665-013-0052-2.

Gao, Z., Liu, Y., Dong, J., 2018. Traditional Chinese medicine tonifying kidney therapy (Bu shen) for stable chronic obstructive pulmonary disease: protocol for a systematic review and meta-analysis. Medicine (Baltim.) 97, e13701. https://doi.org/10.1097/md.0000000000013701.

He, M., Lippestad, M., Li, D., et al., 2018. Activation of the EGF receptor by histamine receptor subtypes stimulates mucin secretion in conjunctival goblet cells. Invest. Ophthalmol. Vis. Sci. 59, 3543–3553. https://doi.org/10.1167/iovs.18-2476.

Jia, Z., Bao, K., Wei, P., et al., 2020. EGFR activation-induced decreases in claudin1 promote MUC5AC expression and exacerbate asthma in mice. Mucosal Immunol. https://doi.org/10.1038/s41385-020-0272-z.

Jiang, Y., David, B., Tu, P., et al., 2010. Recent analytical approaches in quality control of traditional Chinese medicines–a review. Anal. Chim. Acta 657, 9–18. https://doi.org/10.1016/j.aca.2009.10.024.

Kalyuzhin, O.V., 2018. Effect of N-acetylcysteine on mucosal immunity of respiratory tract. Ter. Arkh. 90, 89–95. https://doi.org/10.26442/terarkh201890389-95.

Kesimer, M., Ford, A.A., Ceppe, A., et al., 2017. Airway mucin concentration as a marker of chronic bronchitis. N. Engl. J. Med. 377, 911–922. https://doi.org/10.1056/NEJMoa1701632.

Li, J., Li, S.Y., Yu, X.Q., et al., 2012. Bu-Fei Yi-Shen granule combined with acupoint sticking therapy in patients with stable chronic obstructive pulmonary disease: a randomized, double-blind, double-dummy, active-controlled, 4-center study. J. Ethnopharmacol. 141, 584–591. https://doi.org/10.1016/j.jep.2011.08.060.

Li, J., Li, Y., Li, S., et al., 2012. Long-term effects of Tiaobu Feishen therapies on systemic and local inflammation responses in rats with stable chronic obstructive pulmonary disease. Zhong Xi Yi Jie He Xue Bao 10, 1039–1048. https://doi.org/10.3736/

jcim20120913.
Li, J., Yang, L., Yao, Q., et al., 2014. Effects and mechanism of bufei yishen formula in a rat chronic obstructive pulmonary disease model. Evid. base Compl. Alternative Med., 381976. https://doi.org/10.1155/2014/381976. 2014.
Li, J., Zhao, P., Li, Y., et al., 2015. Systems pharmacology-based dissection of mechanisms of Chinese medicinal formula Bufei Yishen as an effective treatment for chronic obstructive pulmonary disease. Sci. Rep. 5, 15290. https://doi.org/10.1038/srep15290.
Li, S., Li, J., Wang, M., et al., 2012. Effects of comprehensive therapy based on traditional Chinese medicine patterns in stable chronic obstructive pulmonary disease: a four-center, open-label, randomized, controlled study. BMC Compl. Alternative Med. 12, 197. https://doi.org/10.1186/1472-6882-12-197.
Li, Y., Li, J.S., Li, W.W., et al., 2014. Long-term effects of three Tiao-Bu Fei-Shen therapies on NF-kappaB/TGF-beta1/smad2 signaling in rats with chronic obstructive pulmonary disease. BMC Compl. Alternative Med. 14, 140. https://doi.org/10.1186/1472-6882-14-140.
Li, Y., Li, S.Y., Li, J.S., et al., 2012. A rat model for stable chronic obstructive pulmonary disease induced by cigarette smoke inhalation and repetitive bacterial infection. Biol. Pharm. Bull. 35, 1752–1760. https://doi.org/10.1248/bpb.b12-00407.
Liu, W., Zhang, X., Mao, B., et al., 2020. Systems pharmacology-based study of Tanreqing injection in airway mucus hypersecretion. J. Ethnopharmacol. 249, 112425. https://doi.org/10.1016/j.jep.2019.112425.
Livraghi-Butrico, A., Grubb, B.R., Wilkinson, K.J., et al., 2017. Contribution of mucus concentration and secreted mucins Muc5ac and Muc5b to the pathogenesis of muco-obstructive lung disease. Mucosal Immunol. 10, 829. https://doi.org/10.1038/mi.2017.29.
Lu, X., Li, Y., Li, J., et al., 2016. Sequential treatments with Tongsai and bufei yishen granules reduce inflammation and improve pulmonary function in acute exacerbation-risk window of chronic obstructive pulmonary disease in rats. Evid. base Compl. Alternative Med., 1359105. https://doi.org/10.1155/2016/1359105. 2016.
Ma, J., Tian, Y., Li, J., et al., 2019. Effect of bufei yishen granules combined with electroacupuncture in rats with chronic obstructive pulmonary disease via the regulation of TLR-4/NF-kappaB signaling. Evid. base Compl. Alternative Med., 6708645. https://doi.org/10.1155/2019/6708645. 2019.
Okuda, K., Chen, G., Subramani, D.B., et al., 2019. Localization of secretory mucins MUC5AC and MUC5B in normal/healthy human airways. Am. J. Respir. Crit. Care Med. 199, 715–727. https://doi.org/10.1164/rccm.201804-0734OC.
Patel, A.R., Patel, A.R., Singh, S., et al., 2019. Global initiative for chronic obstructive lung disease: the changes made. Cureus 11, e4985. https://doi.org/10.7759/cureus.4985.
Ramos, F.L., Krahnke, J.S., Kim, V., 2014. Clinical issues of mucus accumulation in COPD. Int. J. Chronic Obstr. Pulm. Dis. 9, 139–150. https://doi.org/10.2147/copd.S38938.
Sheaffer, K.L., Updike, D.L., Mango, S.E., 2008. The Target of Rapamycin pathway antagonizes pha-4/FoxA to control development and aging. Curr. Biol. 18, 1355–1364. https://doi.org/10.1016/j.cub.2008.07.097.
Shen, Y., Huang, S., Kang, J., et al., 2018. Management of airway mucus hypersecretion in chronic airway inflammatory disease: Chinese expert consensus (English edition). Int. J. Chronic Obstr. Pulm. Dis. 13, 399–407. https://doi.org/10.2147/copd.S144312.
Song, W.Y., Song, Y.S., Ryu, H.W., et al., 2017. Tilianin inhibits MUC5AC expression mediated via down-regulation of EGFR-MEK-ERK-sp1 signaling pathway in NCI-H292 human airway cells. J. Microbiol. Biotechnol. 27, 49–56. https://doi.org/10.4014/jmb.1610.10012.
Tagaya, E., Yagi, O., Sato, A., et al., 2016. Effect of tiotropium on mucus hypersecretion and airway clearance in patients with COPD. Pulm. Pharmacol. Therapeut. 39, 81–84. https://doi.org/10.1016/j.pupt.2016.06.008.
Tian, Y., Li, J., Li, Y., et al., 2016. Effects of bufei yishen granules combined with acupoint sticking therapy on pulmonary surfactant proteins in chronic obstructive pulmonary disease rats. BioMed Res. Int., 8786235. https://doi.org/10.1155/2016/8786235. 2016.
Tian, Y., Li, Y., Li, J., et al., 2017. Bufei yishen granules combined with acupoint sticking therapy suppress inflammation in chronic obstructive pulmonary disease rats: via JNK/p38 signaling pathway. Evid. base Compl. Alternative Med., 1768243. https://doi.org/10.1155/2017/1768243. 2017.
Tian, Y., Li, Y., Li, J., et al., 2015. Bufei Yishen granule combined with acupoint sticking improves pulmonary function and morphormetry in chronic obstructive pulmonary disease rats. BMC Compl. Alternative Med. 15, 266. https://doi.org/10.1186/s12906-015-0787-0.
Wang, C., Xu, J., Yang, L., et al., 2018. Prevalence and risk factors of chronic obstructive pulmonary disease in China (the China Pulmonary Health [CPH] study): a national cross-sectional study. Lancet 391, 1706–1717. https://doi.org/10.1016/s0140-6736(18)30841-9.
Wang, H., Zhang, H., Li, J., et al., 2015. Effectiveness and safety of traditional Chinese medicine on stable chronic obstructive pulmonary disease: a systematic review and meta-analysis. Compl. Ther. Med. 23, 603–611. https://doi.org/10.1016/j.ctim.2015.06.015.
Wang, J., Ren, D., Sun, Y., et al., 2020. Inhibition of PLK4 might enhance the anti-tumour effect of bortezomib on glioblastoma via PTEN/PI3K/AKT/mTOR signalling pathway. J. Cell Mol. Med. https://doi.org/10.1111/jcmm.14996.
Wang, J., Zhu, M., Wang, L., et al., 2019. Amphiregulin potentiates airway inflammation and mucus hypersecretion induced by urban particulate matter via the EGFR-PI3Kalpha-AKT/ERK pathway. Cell. Signal. 53, 122–131. https://doi.org/10.1016/j.cellsig.2018.10.002.
Whitsett, J.A., 2018. Airway epithelial differentiation and mucociliary clearance. Ann Am Thorac Soc 15https://doi.org/10.1513/AnnalsATS.201802-128AW. S143-s48.
Zhao, P., Li, J., Li, Y., et al., 2015. Systems pharmacology-based approach for dissecting the active ingredients and potential targets of the Chinese herbal Bufei Jianpi formula for the treatment of COPD. Int. J. Chronic Obstr. Pulm. Dis. 10, 2633–2656. https://doi.org/10.2147/copd.S94043.
Zhao, P., Li, J., Tian, Y., et al., 2018. Restoring Th17/Treg balance via modulation of STAT3 and STAT5 activation contributes to the amelioration of chronic obstructive pulmonary disease by Bufei Yishen formula. J. Ethnopharmacol. 217, 152–162. https://doi.org/10.1016/j.jep.2018.02.023.
Zhou-Suckow, Z., Duerr, J., Hagner, M., et al., 2017. Airway mucus, inflammation and remodeling: emerging links in the pathogenesis of chronic lung diseases. Cell Tissue Res. 367, 537–550. https://doi.org/10.1007/s00441-016-2562-z.